

Computation of vertical velocity incorporating release of latent heat of condensation

K. V. RAO and S. RAJAMANI

Indian Institute of Tropical Meteorology, Poona

ABSTRACT. The vorticity equation for geostrophic motion, the thermodynamic energy equation and the equation of continuity for moisture have been used to compute vertical velocities taking into account the release of latent heat of condensation. Computations by this model in the case of a synoptic situation show that incorporation of latent heat release in the model increases considerably the magnitude of upward vertical velocity at all levels where condensation takes place. The effects of friction and topography are discernible only at 1000 mb and 850-mb levels.

1. Introduction

Rao and Rajamani (1970) had computed vertical velocities in the field of a monsoon depression by means of the ω -equation with the assumption of adiabatic motion. They had also drawn attention to the feature pointed out by Danard (1966), viz., the inclusion of latent heat in the ω -equation would result in an increase in the magnitude of the computed vertical motion. In this paper, vertical velocity has been computed after including latent heat of condensation on lines similar to those of Eugene Aubert (1957). Recently a number of workers (Japanese workers 1965, Krishnamurti 1968, Haltiner 1971) have parameterised the latent heat release by incorporating this effect in the static stability parameter. The method of Eugene Aubert was however followed, as the authors considered it to be direct and based on actual observations. Also, the effects of topography and friction have been incorporated, by modifying the lower boundary condition.

2. List of symbols

V_0	Surface wind speed
V	Geostrophic wind velocity
ζ	Relative vorticity
f_0	Standard value for the Coriolis parameter
ϕ	Geopotential
z	Height in metres of an isobaric surface
σ	Static stability
θ	Potential temperature
α	Specific volume

∇	Isobaric gradient operator
	$\left(i \frac{\partial}{\partial x} + j \frac{\partial}{\partial y} \right)$
∇^2	Laplacian operator
	$\left(\frac{\partial^2}{\partial x^2} + \frac{\partial^2}{\partial y^2} \right)$
$J(A, B)$	Jacobian operator
	$\left(\frac{\partial A}{\partial x} \frac{\partial B}{\partial y} - \frac{\partial A}{\partial y} \frac{\partial B}{\partial x} \right)$
R	Specific gas constant for dry air
c_p	Specific heat of air at constant pressure
p	Pressure
dQ/dt	Rate of change of heat
q	Specific humidity
q_s	Saturation specific humidity
L	Latent heat of condensation of water vapour
ω_s	Adiabatic vertical velocity
ω_m	Vertical velocity due to the term incorporating release of latent heat
ω	Total vertical velocity (including all effects)
T_v	Virtual temperature
T	Temperature
R_w	Specific gas constant for water vapour
ϵ	Ratio of the gas constant for water vapour to that for dry air
ρ	Density of air
C_D	Drag coefficient
g	Acceleration due to gravity
c	Rate of condensation of water vapour per unit volume.

3. Basic equations

The equations that were used are:

The geostrophic vorticity equation

$$\frac{\partial \zeta}{\partial t} + \mathbf{V} \cdot \nabla (\zeta + f) = f_0 \frac{\partial \omega}{\partial p} \quad (1)$$

The thermodynamic energy equation

$$\begin{aligned} \frac{\partial}{\partial t} \left(\frac{\partial \phi}{\partial p} \right) + \mathbf{V} \cdot \nabla \left(\frac{\partial \phi}{\partial p} \right) + \sigma \omega \\ = - \frac{R}{c_p p} \frac{dQ}{dt} \end{aligned} \quad (2)$$

The continuity equation for specific humidity

$$\frac{\partial q}{\partial t} + \mathbf{V} \cdot \nabla q + \omega \frac{\partial q}{\partial p} + \frac{c}{\rho} = 0 \quad (3)$$

Eq. (3) is used in two forms; when q is greater than q_s

$$\begin{aligned} \left[q_s(t + \Delta t) - q(t - \Delta t) \right] / 2 \Delta t + \left(\mathbf{V} \cdot \nabla q \right)_t + \\ \left(\omega \frac{\partial q}{\partial p} \right)_t = - \frac{c}{\rho} \end{aligned} \quad (3a)$$

When q is less than q_s ,

$$\begin{aligned} \left[q(t + \Delta t) - q(t - \Delta t) \right] / 2 \Delta t + \left(\mathbf{V} \cdot \nabla q \right)_t \\ + \left(\omega \frac{\partial q}{\partial p} \right)_t = 0 \end{aligned} \quad (3b)$$

In (2) we can substitute $L(c/\rho)$ for dQ/dt incorporating latent heat of condensation. The quasi-geostrophic ω equation can be derived from (1) and (2) as

$$\begin{aligned} \sigma \nabla^2 \omega + f_0^2 \frac{\partial^2 \omega}{\partial p^2} = f_0 \frac{\partial}{\partial p} \left[\mathbf{V} \cdot \nabla (\zeta + f) \right. \\ \left. - \nabla^2 \left[\mathbf{V} \cdot \nabla \left(\frac{\partial \phi}{\partial p} \right) \right] - \frac{RL}{c_p P} \nabla^2 \left(\frac{c}{\rho} \right) \right] \end{aligned} \quad (4)$$

The equation for height tendency is

$$\begin{aligned} \nabla^2 \frac{z}{\partial t} = -J \left[z, \left(\frac{g}{f_0} \nabla^2 z + f \right) \right] \\ + \frac{f_0^2}{g} \frac{\partial^2 \omega}{\partial p^2} \end{aligned} \quad (5)$$

Forward differencing scheme was used to get the forecast height after the first time step.

$$z_1 = z_0 + \left(\frac{\partial z}{\partial t} \right)_0 \quad (6)$$

where the numerical suffixes indicate the time step.

Eq. (4) may be split up to compute the adiabatic vertical velocity ω_d (ω -dry) and the vertical velocity ω_m (ω -moist) which results from release of latent heat of condensation. Thus,

$$\begin{aligned} \sigma \nabla^2 \omega_d + f_0^2 \frac{\partial \omega_d}{\partial p^2} = f_0 \frac{\partial}{\partial p} \\ \left[\mathbf{V} \cdot \nabla (\zeta + f) \right] - \nabla^2 \left[\mathbf{V} \cdot \nabla \left(\frac{\partial \phi}{\partial p} \right) \right] \end{aligned} \quad (7a)$$

$$\sigma \nabla^2 \omega_m + f_0^2 \frac{\partial^2 \omega_m}{\partial p^2} = - \frac{RL}{c_p p} \nabla^2 \left(\frac{c}{\rho} \right) \quad (7b)$$

$$\text{Total } \omega = \omega_d + \omega_m \quad (7c)$$

4. Computations

The same synoptic situation at 12 GMT on 25 July 1966 as was studied in the earlier investigation (Rao and Rajamani 1970) was considered. The height values at grid points on 1000, 850, 700, 500, 300 and 150 mb surfaces were used. Isopleths for q on 1000, 850, 700, 500 mb surfaces were also drawn up and the grid point values (at 2 degree intervals) were read off and used for q . The upper boundary conditions for ω was taken to be zero at 150 mb surface. However, the value for ω at 1000 mb due to friction and topography was computed and used as the lower boundary condition.

The procedure developed by Gambo *et al.* (1956) was followed for computing vertical velocity due to topography. The grid point values of topography were taken from the publication by Berkofsky and Bertoni (1960). The expression adopted for computing vertical velocity due to friction (Haltiner 1971) is

$$\omega_f = \frac{g}{f_0} \left[\frac{\partial}{\partial y} \left(\rho C_D u_0 V_0 \right) - \frac{\partial}{\partial x} \left(\rho C_D v_0 V_0 \right) \right]$$

where C_D the drag coefficient has a value 2.5×10^{-3} (Krishnamurti 1968) and the surface wind $V\alpha$ is computed from the expression $V_0 = V (\cos \alpha \sin \alpha)$. The angle of inflow has been assumed to be 20° . The computational scheme is indicated below:

1. $t=0$ Input values z, q
2. $t=0$ Compute ω_d from Eq. 7(a)
3. $t=t+\Delta t$ (i) Compute $z_{t+\Delta t}$ from (5) and (6)
 - (ii) Compute T_v, T, q_s (see Appendix)
 - (iii) Compute c/ρ from Eq. 3(a)
 - (iv) Compute q from Eq. 3(b)
4. Compute ω_m from Eq. 7(b)
5. Compute total ω from Eq. 7(c)

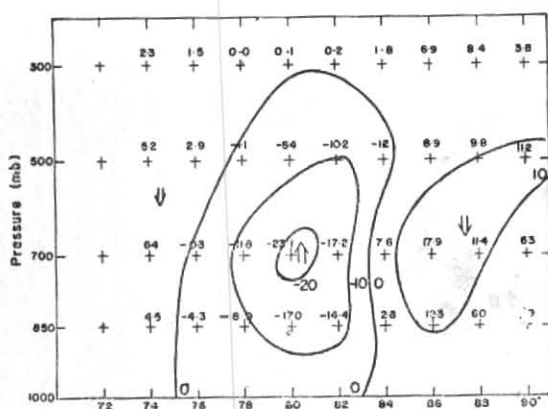


Fig. 1(a). Vertical cross section (at 18°N) of vertical velocity without friction, topography and moisture (ω in units of 10^{-4} mb/sec)

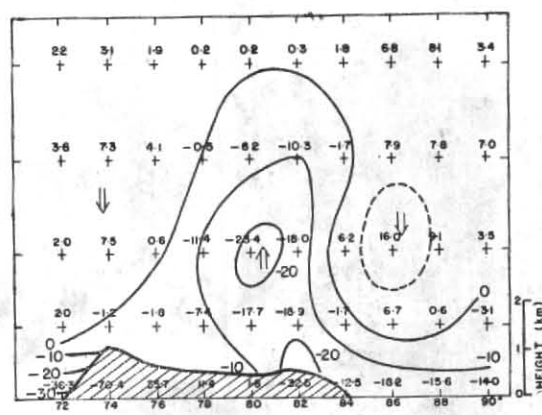


Fig. 1(b). Vertical cross section (at 18°N) of vertical velocity with friction and topography but without moisture (ω in units of 10^{-4} mb/sec)

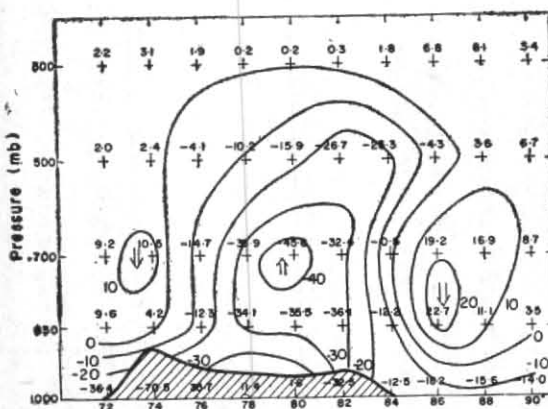


Fig. 1(c). Vertical cross section (at 18°N) of vertical velocity with friction, topography and moisture (ω in units of 10^{-4} mb/sec)

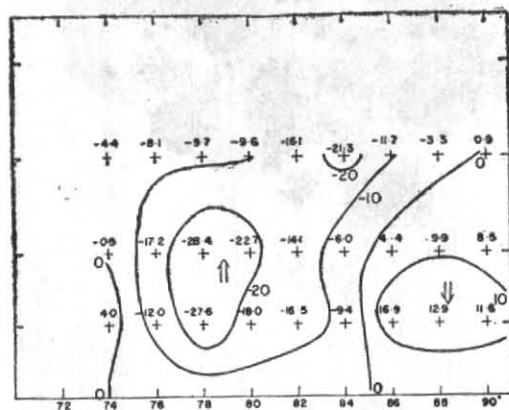


Fig. 1(d). Vertical cross section (at 18°N) of contribution due to moisture (ω_m in units of 10^{-4} mb/sec)

b. Discussion of the results

(a) The vertical cross sections of ω at grid points along Lat. 18°N are presented in Figs. 1(a) to 1(d). Fig. 1(a) gives the adiabatic vertical motion with the lower boundary condition being $\omega=0$ at 1000 mb, *i.e.*, the effects of friction and topography have not been incorporated in the lower boundary condition.

Fig. 1(b) gives adiabatic vertical velocity in which the effects of friction and topography have been incorporated in the lower boundary condition.

Fig. 1(c) shows vertical velocity in which the effect of release of latent heat of condensation of water vapour has been incorporated. This also takes into account the effects of friction and topography in the lower boundary condition. Lastly, Fig. 1(d) indicates the contribution to vertical velocity by the latent heat released due to condensation.

From comparison of Figs. 1(a) and 1(b) it is seen that at levels 850 to 300 mb there is no significant difference in the values of vertical velocity. However in Fig. 1(b) at 1000 mb level where the contributions due to topography and friction have been computed, it is seen that at the grid points 72° and 74° E, the westward slope of the Western Ghats gives rise to upward vertical motion while on the eastward slopes downward vertical motion is induced upto grid point 80°E. It is of interest to note that at the grid point at 74°E where the topography profile has a peak, the vertical motion due to topography is also maximum. Right at the surface (1.07 km) the vertical velocity is about -50×10^{-4} mb/sec and this value increases to -70×10^{-4} mb/sec at 1000 mb due to linear extrapolation.

The upward vertical motion from 82° to 90°E is due to the frictional effect. It is interesting to note that friction and topography affect 1000-mb level and their effects are, however, small at 850-mb level and negligible at higher levels, *viz.*, 700, 500 and 300-mb levels.

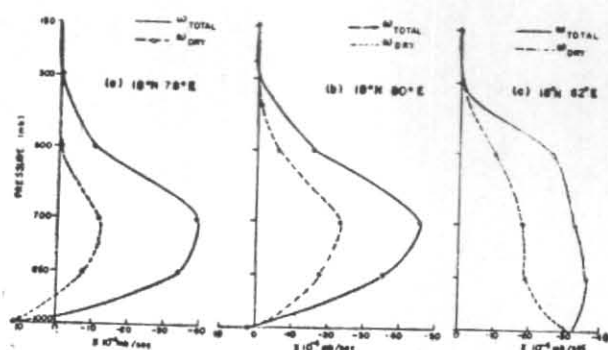


Fig. 2. Vertical profiles of ω_{TOTAL} and ω_{DRY} (a) at $18^\circ N$ $78^\circ E$, (b) $18^\circ N$ $80^\circ E$ and (c) $18^\circ N$ $82^\circ E$

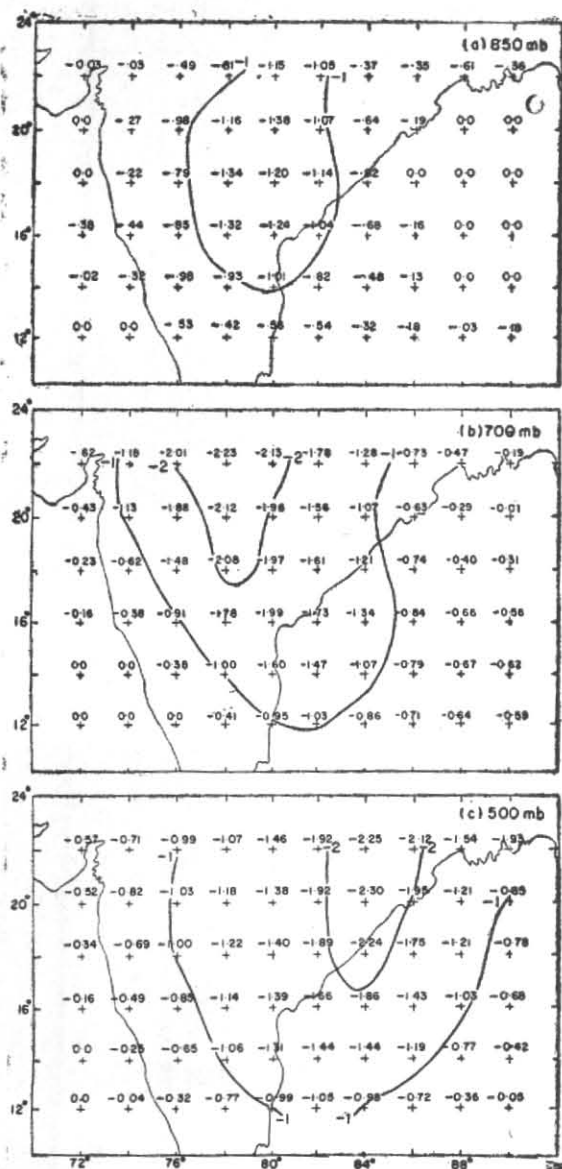


Fig. 3 c/p at 850 mb, 700 mb and 500-mb levels ($\times 10^{-3} \text{ Sec}^{-1}$)

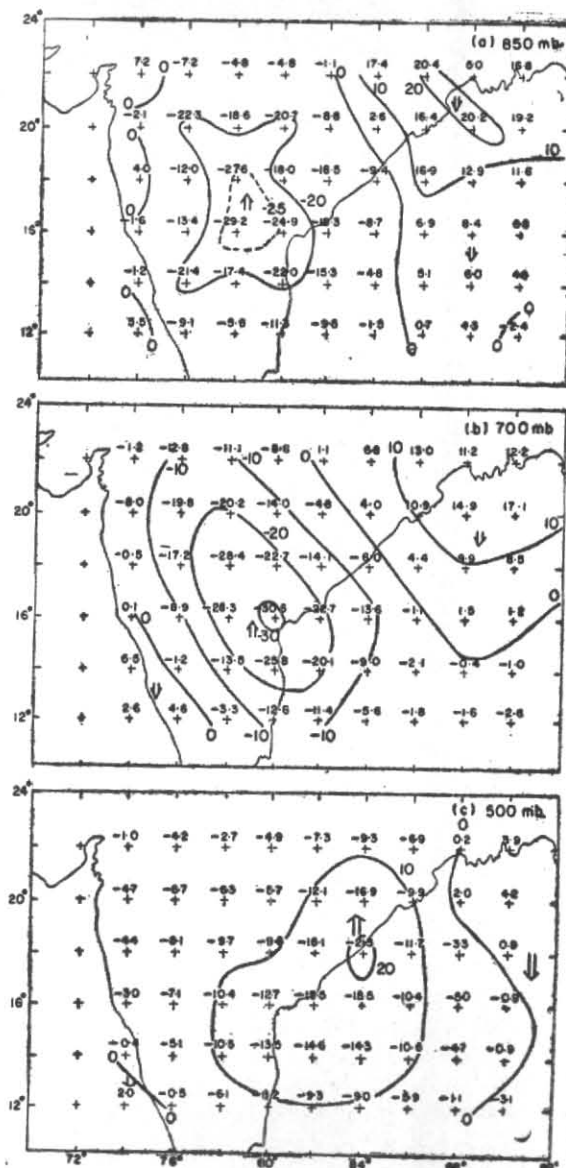


Fig. 4 Contribution due to moisture ω at 850 mb, 700 mb and 500-mb levels (in units of $10^{-4} m$)

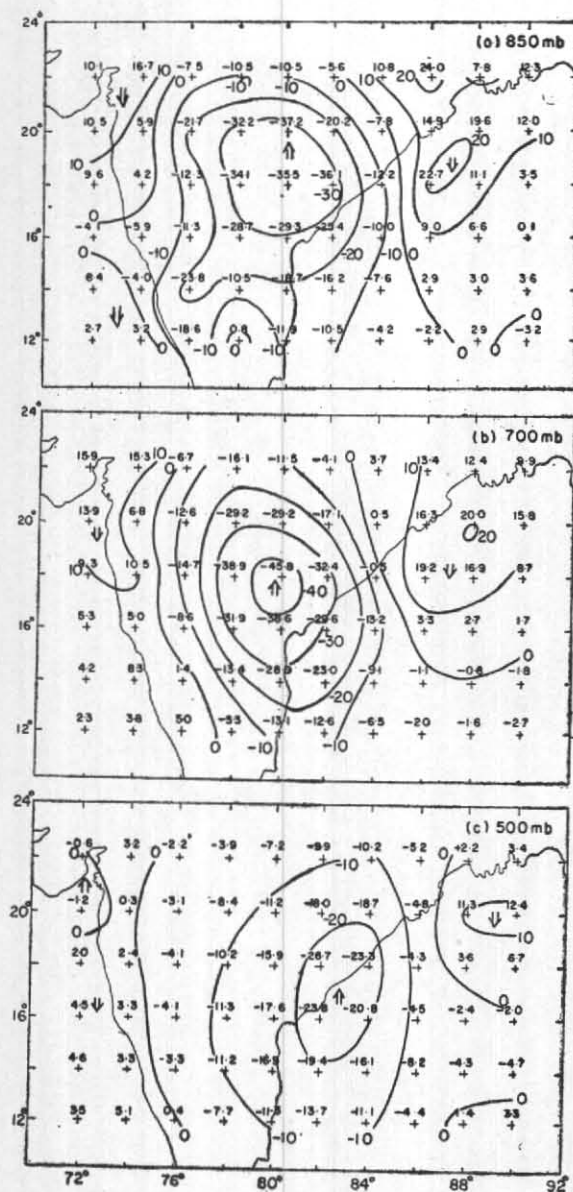


Fig. 5. Total vertical velocity at 850 mb, 700 mb and 500-mb levels. Friction, topography and moisture included. (ω in units of 10^{-4} mb/sec)

When Figs. 1(b), 1(c) and 1(d) are compared, it is immediately apparent that the contribution to vertical velocity due to the release of latent heat is considerable and of the same order of magnitude as the adiabatic vertical motion. The upward vertical motion at 500-mb level is not only increased but its horizontal extent has also increased. At 700 mb, at the grid point 18°N and 80°E the adiabatic vertical motion is -23×10^{-4} mb/sec, whereas the vertical motion in the moist model is -48×10^{-4} mb/sec. To illustrate this point the vertical profile at grid points 18°N , 78°E , 18°N , 80°E and 18°N , 82°E are given in Fig. 2.

(b) *Fields of c/ρ , ω_m and total ω* —The ratio c/ρ is computed from Eq. 3(a). As suggested by Smagorinsky (1960) the condensation criterion was set to 80 per cent instead of 100 per cent. When actual specific humidity at any time is greater than $0.8 q_s$, (saturation specific humidity) the condensation is assumed to take place and equation 3(a) is used to compute c/ρ . The reason for the reduced criterion is that we are concerned with gross humidity which is a space average quantity. With finite grid size the upper limit of relative humidity need not be 100 per cent for condensation to take place.

The fields of c/ρ at 850, 700 and 500 mb are presented in Fig. 3. The negative sign denotes sinks of water vapour, *i.e.*, condensation of water vapour takes place at those points. Positive values are absent, as no source of water vapour has been considered, *i.e.*, evaporation of water was not considered in the model. At 850-mb level there are few points with zero values thereby indicating that condensation did not take place at those points. There is small region between 76°E to 84°E covered by the isopleth of value -1 for c/ρ . At 700 and 500-mb levels the isopleth of value -1 occupies a larger area within which there is a small region covered by the isopleth of value -2 . This may be due to the fact that lower temperatures at 700 mb and 500-mb levels may facilitate condensation of water vapour.

Fig. 4 gives the vertical velocity ω_m computed from the term incorporating the latent heat release due to condensation alone. On comparison of these figures with the corresponding figures in Fig. 3, it is seen that large values of upward motion occur generally in regions close to regions where c/ρ is large, though they may not coincide. This feature may be due to the reason that computation of ω_m from c/ρ involves calculation of Laplacian and three dimensional relaxation of the forcing function due to c/ρ . These two factors are also responsible for occurrence of downward motion at those grid points where c/ρ is zero and hence one would expect ω_m to be zero as there is no condensation taking place.

The patterns of total vertical velocity ω at 850, 700 and 500 mb levels, after incorporation of the effects due to release of latent heat, topography and friction are given in Fig. 5.

On comparison of these patterns with the pattern of vertical velocity due to adiabatic motion without the effect of friction and topography, the following main features are brought out:

1. The inclusion of the three effects makes the patterns slightly irregular especially at 850-mb level.

2. The magnitudes of upward motion are increased considerably at all the three levels, viz., 850, 700 and 500 mb due to incorporation of latent heat release.

3. The contribution due to friction and topography is discernible only at lower levels, i.e., at 1000 and 850 mb and is negligible at 700-mb level and above.

Acknowledgements

The authors wish to express their gratitude to Dr. Bh.V. Ramana Murty for his kind interest and encouragement. They wish to thank Shri K. Krishna for helpful discussions. Thanks are also due to Shri A. Girijavallabhan for typing the manuscript and the members of the Drawing and Photography Units for the preparation of diagrams.

REFERENCES

- | | | |
|---|------|--|
| Aubert, Eugene J. | 1957 | <i>J. Met.</i> , 14 , 6, pp. 527-542. |
| Berry, F. A. Bolla, E. and Beers, N. R. | 1945 | <i>Hand book of Meteorology</i> , McGraw-Hill Book Co. |
| Blackadar, A. K. | 1967 | Rep. on Global Atmospheric Research Programme, Appendix IV. |
| Danard, M. B. | 1966 | <i>J. appl. Met.</i> , 5 , 1, pp. 85-93 |
| Gambo, K., Saito, N., Fujiwara, S. and Murakami, T. | 1956 | <i>J. met. Soc., Japan</i> , 34 , 5, pp. 254-265. |
| Haltiner, G. J. | 1971 | <i>Numerical Weather Prediction</i> , John Willey & Sons. |
| Krishnamurti, T. N. | 1968 | <i>Mon. Weath. Rev.</i> , 9 , 4, pp. 197-207. |
| Lettau, H. H. | 1959 | <i>Advances in Geophysics</i> , 6 , pp. 241-258. |
| Rao, K.V. and Rajamani, S. | 1970 | <i>Indian J. Met. Geophys.</i> , 21 , 2, pp. 187-194. |
| Smagorinsky, J. | 1960 | <i>Geophys. Monogr.</i> , 5 , Amer. Geophys. Un. pp. 71-78. |
| Staff Members, Electronic Computers Centre | 1965 | <i>J. met. Soc. Japan</i> , 43 , 5, pp. 246-261. |
| Berkofsky, L. and Bertoni, E. A. | 1960 | Topographic charts at one degree intersections for the entire earth. Res. Notes, 42 , G.R.D., U.S.A.F., Mass., p. 43. |
| Smithsonian Institution, Washington | 1963 | <i>Smithsonian Meteorological Tables</i> , 6th Rev. Ed. |

APPENDIX

Drag coefficient

It is appropriate to use the geostrophic drag coefficient C_{Dg} as defined by Lattau (1959) in the computation, as the winds have been computed from the geostrophic wind equation.

$$\begin{aligned} \text{The surface stress } \tau_0 &= \rho u_*^2 \\ &= \rho C_D u_a^2 = \rho C_{Dg} u_g^2 \end{aligned}$$

where

- u_* = frictional velocity
- u_g = geostrophic wind
- u_a = wind speed at anemometer level
- C_D = surface drag coefficient,
- C_{Dg} = geostrophic drag coefficient

From this relation, $C_D = (u_*/u_a)^2$ and $C_{Dg} = (u_*/u_g)^2$. Observations indicate a typical magnitude of 40 for u_g/u_* (Blackadar 1967), so that

$$C_{Dg} \approx \left(\frac{1}{40} \right)^2 \approx 0.625 \times 10^{-3}$$

In our computation, our assumption of a value of 20° for the angle of inflow and a value of 2.5×10^{-3} for surface drag coefficient C_D is equivalent to a value of 0.9×10^{-3} for geostrophic coefficient, which is justifiable.

1. $T_v = \left(\frac{z_1 - z_2}{R} \right) g \ln \frac{p_1}{p_2}$
2. $T = T_v \left(\frac{1 + q}{1 + q/\epsilon} \right)$, $\epsilon = 0.62197$
3. Vapour pressures at temperature $t^\circ\text{C}$ given by

$$e_s = 6.11 \times 10^{at/(b+t)}$$
 where, $a = 7.5$, $b = 237.5$
(Berry, Bolla and Beers 1945)
4. $q_s = \frac{0.62197 f_w e_s}{p - f_w e_s}$

where the correction factor $f_w = 1.005$
(*Smithsonian Meteorological Tables* 1963)